**J. J. Blech**
Faculty of Mechanical Engineering.

**I. Green**
Faculty of Mechanical Engineering.

**J. Kopelman**
Department of Food Engineering and Biotechnology.

Technion,
Israel Institute of Technology,
Haifa 32000, Israel

# Transient Temperature Distribution in Partially Filled Rotating Horizontal Cylinders

*The transient temperature distribution in an infinitely long horizontal rotating cylinder which is partially filled by a viscous fluid is calculated. Thermal boundary and initial conditions are such that the fluid starts from a uniform temperature, and that the outer boundary (cylinder surface) is isothermal at a different temperature. Nondimensional analysis shows that the problem can be fully described by a properly defined Fourier modulus and a normalized bubble eccentricity.*

## Introduction

The internal temperature distribution in a partially filled cylinder rotating about its axis and being exposed to an external heat source has several applications, one of those being in the food processing industry where liquid canned foods may be pasteurized while rotating horizontally and moved by some conveyor through a steam chamber. The liquids partially fill the can, and there exists a headspace with trapped air. During rotation of the can about its axis, the air bubble mixes the contents of the can, thus accelerating the heating process. In spite of the wide usage of induced convection heating in the food industry, the theoretical analysis of flow and heat, useful for a systematic design of sterilization processes, is quite limited (Lenz and Lund, 1978). Gavish et al. (1978) attacked the flow problem in the can, but due to the complexity of the problem they had to restrict their analysis to infinitely long cylinders with cylindrical bubbles, as opposed to the actual problem of finite cylinders with bubbles resembling an airfoil in their cross section. The purpose of this analysis is to extend the flow problem, which was attacked in Gavish et al. (1978), and determine the transient temperature field in this configuration.

## Analysis

The incompressible viscous flow in a partially filled rotating horizontal cylinder was studied both experimentally and theoretically by Gavish et al. (1978). Here we propose to study the transient temperature distribution in that field under the assumption that both fields are decoupled.

Maintaining only convection-conduction terms in the energy equation leads to:

$$\frac{\partial T}{\partial t}+\mathrm{Pe}\vec{U}\cdot\nabla\bar{T}=\nabla^2 T \tag{1}$$

where $T$, $\vec{U}$, and $\alpha$ are the fluid temperature, velocity, and thermal diffusivity, respectively. Pe is the Peclet number, $r_2^2\Omega/\alpha$, with $r_2$ and $\Omega$ being the cylinder outer radius and its angular velocity, respectively.

A typical time scale is of order $0(r_2{}^2/\alpha)$. The Peclet number gives a measure of the ratio between typical times for convection and conduction. In the problem of our interest it turns out that Pe >> 1 (Pe ~ $10^5$). Such a large Peclet number discards the possibility of solving equation (1) by an ordinary finite difference scheme since the norm of the grid must be 1/Pe approximately, making it necessary to work with enormously large matrices. We make use, therefore, of the Peclet number being so large by resorting to asymptotic approximations of equation (1).

The solution of the flow problem was given in Gavish et al. (1978), assuming two-dimensional creeping flow. (The variation of the Reynolds number, $\Omega r_1^2/\nu$, in the experiments was in the range 0.20–20.) It is most naturally expressed in Bipolar coordinates. For our purpose, however, there exists a more natural system of coordinates $(r,s)$, $r$ being perpendicular to streamlines and $s$ measured along streamlines.

With respect to the transformations between the Cartesian and natural systems $x(r,s)$, $y(r,s)$, the heat transport equation (1) in the natural coordinate system is:

$$\frac{\partial T}{\partial t}+\mathrm{Pe}\,\frac{U(r,s)}{h_2(r,s)}\,\frac{\partial T}{\partial s}=\frac{1}{h_1h_2}\left[\frac{\partial}{\partial r}\left(\frac{h_2}{h_1}\,\frac{\partial T}{\partial r}\right)+\frac{\partial}{\partial s}\left(\frac{h_1}{h_2}\,\frac{\partial T}{\partial s}\right)\right] \tag{2}$$

where $h_1$ and $h_2$ are the metrics of the transformation.

We expand the temperature in a series:

$$T=T_o+\frac{1}{\mathrm{Pe}}\,T_1+\ \ldots . \tag{3}$$

Inserting the expansion into equation (2) and equating coefficients of like powers of Pe gives for the first order:

$$\frac{U}{h_2}\,\frac{\partial T_o}{\partial s}=0;\ \frac{\partial T_i}{\partial t}+\frac{U}{h_2}\,\frac{\partial T_{i+1}}{\partial s}=L[T_i];\ i=0,1,2,\ \ldots \tag{4}$$

From equation (4) we have:

$$T_o=T_o(r,t) \tag{5}$$

where $L$ is the operator which acts on the right-hand side of equation (2). Integrating equation (4) along streamlines, for $i=0$, and noting that conduction times are much larger than convection times, we get:

Contributed by the Applied Mechanics Division for publication in the Journal of Applied Mechanics.

Discussion on this paper should be addressed to the Editorial Department, ASME, United Engineering Center, 345 East 47th Street, New York, N.Y. 10017, and will be accepted until two months after final publication of the paper itself in the Journal of Applied Mechanics. Manuscript received by ASME Applied Mechanics Division, December 11, 1984; final revision, October 9, 1985.

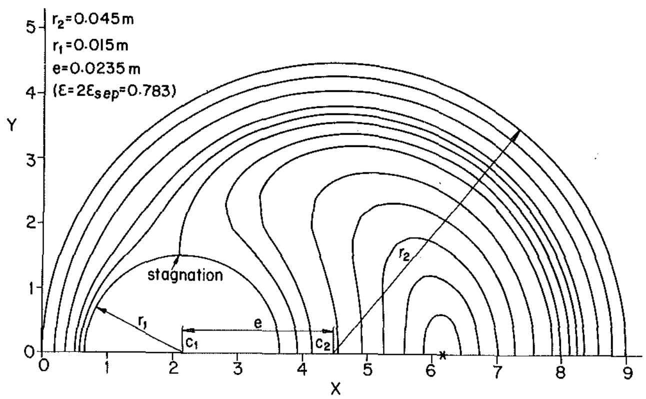


**Fig. 1 Streamlines of the separated flow field for $r_1 = 0.015$ m, $r_2 = 0.045$ m, and $e = 0.0235$ m**

$$\frac{\partial T_o}{\partial t} = \mu_2 \frac{\partial T_o}{\partial r} + \mu_3 \frac{\partial^2 T_o}{\partial r^2} \tag{6}$$

where:

$$\mu_2 = \frac{\gamma_2(r)}{\gamma_1(r)};\ \mu_3 = \frac{\gamma_3(r)}{\gamma_1(r)} \tag{7}$$

and

$$\gamma_1(r) = \int_\psi \frac{h_2}{U} d\sigma;\ \gamma_2(r) = \int_\psi \frac{1}{Uh_1} \frac{\partial}{\partial r}\left(\frac{h_2}{h_1}\right) d\sigma;$$

$$\gamma_3(r) = \int_\psi \frac{h_2}{Uh_1^2}\, d\sigma. \tag{8}$$

Equation (6) is the governing equation in the zeroth order temperature $T_o$. Its physical interpretation is intuitively clear. The temperature distribution $T_o$ is identical to the temperature distribution in a layered solid, its layers being the streamlines. The thermal conductivity of this solid along streamlines is infinite, so that heat flows only in the $r$ direction. The streamlines themselves are isotherms.

## Numerical Formulation

The governing equation (6) is a time dependent partial differential equation in the natural coordinate $r$ only. The complicated dependence of $\mu_2$ and $\mu_3$ on $r$ requires that a numerical method of solution be used. The solution consists of two stages.

**(*a*) Determination of the Flow Field.** The flow field is evaluated by the equations given in Gavish et al. (1978). The simplifying assumptions which were made in Gavish et al. (1978) are summarized below: (*a*) the bubble remains continuous while the cylinder is rotated; (*b*) the cross-sectional shape of the bubble is circular; (*c*) the flow field inside the bubble is negligible, thus the shear stress on the interface is zero; (*d*) the flow is assumed to be a two-dimensional creeping flow. Therefore, the two-dimensional Stokes equations are solved for a bubble location which depends on the angular velocity of the can. At low rotating speeds, the bubble is set far apart from the can center, thus having a high eccentricity, $\epsilon$. The eccentricity is defined by

$$\epsilon = \frac{e}{r_2 - r_1} \tag{9}$$

where $e$ is the distance between the two centers. A typical description of such flow regimes is given in Fig. 1 (streamlines are separated similar to creeping flows around solid cylinders). As the speed increases, the bubble moves toward the can center thus attaining small eccentricities, as described, for example, in Fig. 2, where streamlines are not separated – all of them surround the bubble. Therefore, at small eccentricities, the fluid rotates on one region (see also Fig. 6(*a*) of Gavish et al., 1978). At high eccentricities, the passage between the bubble and the cylinder wall becomes narrow, not permitting all of the fluid to pass through it and thus the fluid engulfs the bubble, forming two rotational regions (see also Figs. 6(*b*), 6(*c*), and 6(*d*) of Gavish et al., 1978).

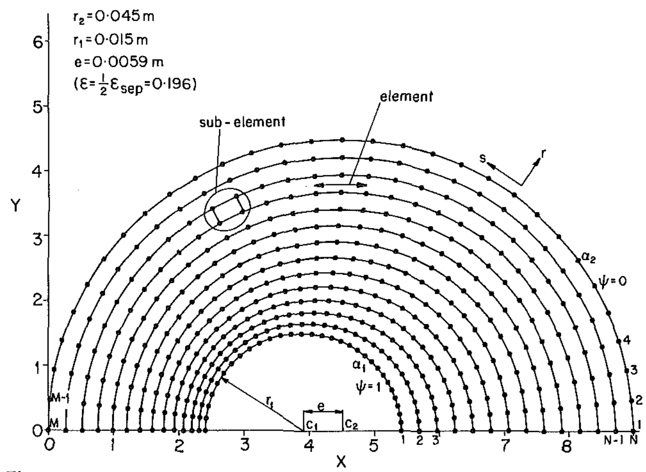


**Fig. 2 Streamlines of the unseparated flow field for $r_1 = 0.015$ m, $r_2 = 0.045$ m, and $e = 0.0059$ m**

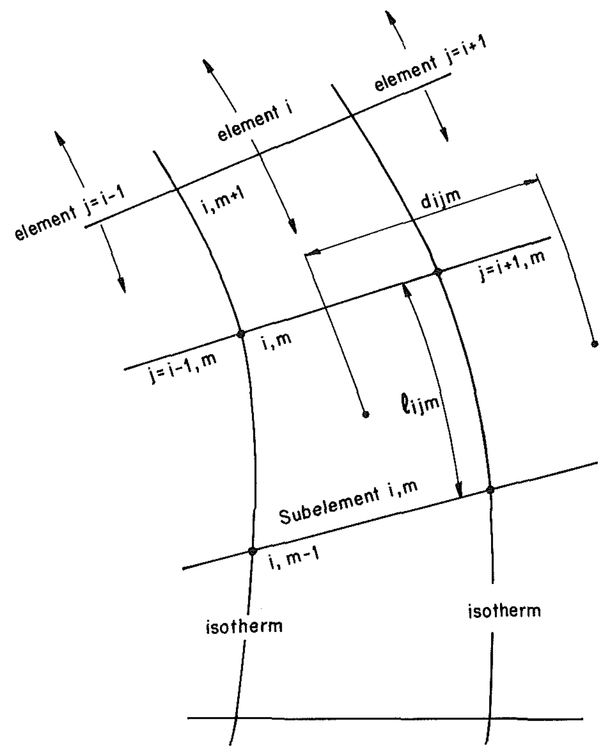


**Fig. 3 Division and nomenclature of elements and subelements**

For the determination of the transient temperature field, the radial and the azimuthal directions are divided into $N-1$ and $M-1$ intervals, respectively. Every four points construct a subelement, and every $M-1$ subelements in the $s$ direction, tangent to streamlines, construct a layer, thus forming $N-1$ layers (elements) in the $r$ direction (see Fig. 2).

**(*b*) Determination of the Transient Temperature Field.** To solve equation (6), a lumped parameters approach is taken, where an energy balance equation is written for each element $i$, which is bounded by two isotherms (streamlines). The resultant equation is

$$T_i^{p+1} = a_i \sum_j S_{ij} T_j^p + b_i T_i^p \tag{10}$$

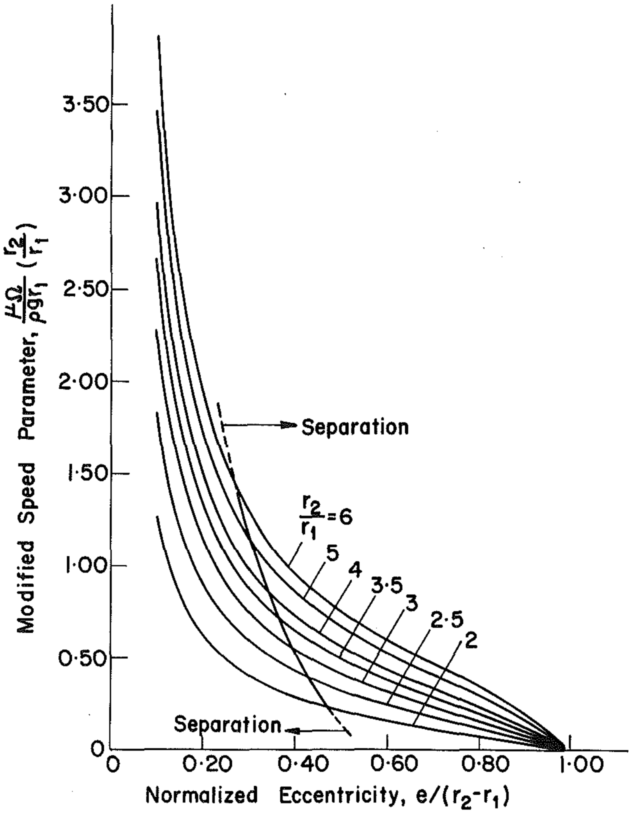


**Fig. 4 Modified speed parameter versus the normalized eccentricity, $\epsilon$, for various radii ratios, $r_2/r_1$**

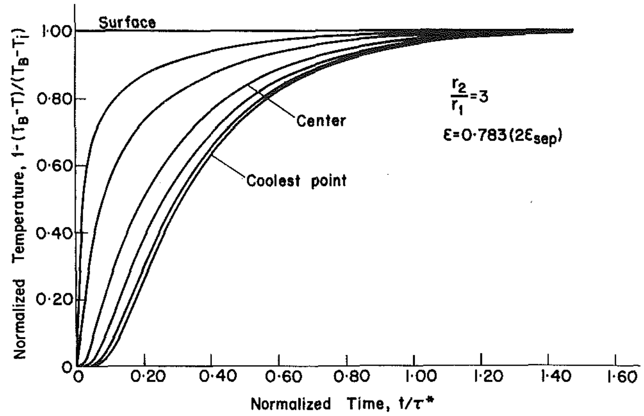


**Fig. 5 Normalized temperature, $\theta$, versus normalized time, $\tau$, for different locations, at $r_2/r_1=3$, and $\epsilon=2\epsilon_{sep}$**

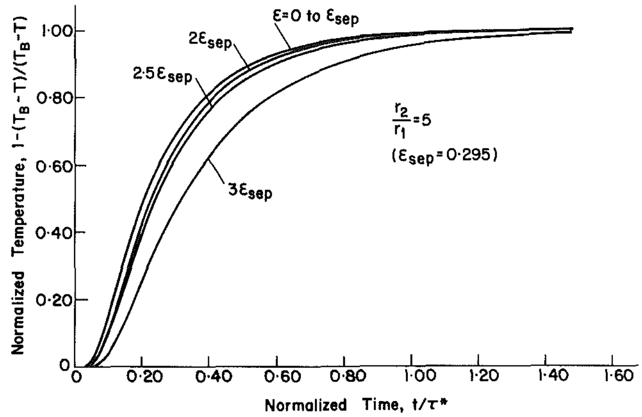


**Fig. 6 Normalized temperature, $\theta$, versus normalized time, $\tau$, for various normalized eccentricities, $\epsilon$, at $r_2/r_1=5$**

where the subscripts on $T$ locate the element and the superscripts refer to time, and

$$a_i=\frac{\Delta t}{C_i};\ b_i=1-\frac{\Delta t}{C_i}\sum_j S_{ij};\ C_i=\rho c_p \Delta A_i \tag{11}$$

$\rho$, $c_p$ are the fluid mass density and specific heat, respectively. $\Delta A_i$ is the area of each element. $S_{ij}$ is the so-called "shape factor" for two adjacent elements, $i$ and $j$:

$$S_{ij}=k\sum_{m=1}^{M-1}\frac{l_{ijm}}{d_{ijm}} \tag{12}$$

where $l_{ijm}$ is the common boundary length of two subelements $m$, located in two adjacent elements $i$ and $j$ (see Fig. 3), and $d_{ijm}$ is the distance between the "centers" of these two subelements.

Numerical stability is guaranteed by requiring $b_i \geq 0$ (thermodynamic reasoning), hence,

$$\Delta t \leq \min\left(\frac{C_i}{\sum_j S_{ij}}\right)_i \quad i=1,2,\ldots,N-1 \tag{13}$$

and time steps where chosen, accordingly, in the program. Based on the above formulation the computer program evaluates first the flow field and divides it into subelements and elements. The program distinguishes between the two flow regimes and identifies all the geometric variables. Then, the temperature in each layer (element) is determined at every time step, subjected to the boundary conditions, $T=T_B$ on the outer surface and $\partial T/\partial r=0$ on the bubble surface. The initial condition for the entire field (excluding the outer boundary) is $T=T_i$.

To obtain a general solution it is necessary to state the problem in a dimensionless form. The governing dimensionless groups which were introduced in Gavish et al. (1978) were regrouped here for more convenience. Figure 4 gives the dependence between the normalized eccentricity, $e/(r_2-r_1)$, and the modified speed parameter, $\mu\Omega(r_2/t_1)/\rho g r_1$, for different $r_2/r_1$ ratios. That figure also gives the eccentricity, $\epsilon_{sep}$, at which separation takes place.

Similarity is also achieved in the temperature field. Let us introduce a time constant, $\tau^*$, based on cylindrical heat transfer, by

$$\tau^*=\frac{r_2^2-r_1^2}{2\alpha}\,\ell n\left(\frac{r_2}{r_1}\right) \tag{14}$$

Defining the Fourier modulus, Fo, by

$$\mathrm{Fo}=\frac{\alpha\tau^*}{r_2{}^2} \tag{15}$$

and substituting (14) in (15) yields:

$$F_0=\frac{1}{2}\left[1-\left(\frac{r_1}{r_2}\right)^2\right]\ell n\left(\frac{r_2}{r_1}\right) \tag{16}$$

Nondimensionalysing further, time, temperature, and the normal coordinate as follows:

$$\tau=\frac{t}{\tau^*};\ \theta=1-\frac{T_B-T}{T_B-T_i};\ R=\frac{r}{r_2} \tag{17}$$

and substituting the above relations in the unidirectional heat conduction equation, which applies here normal to streamlines, results in

$$\frac{\partial\theta}{\partial\tau}=\mathrm{Fo}\,\frac{\partial^2\theta}{\partial R^2} \tag{18}$$

along with the boundary conditions

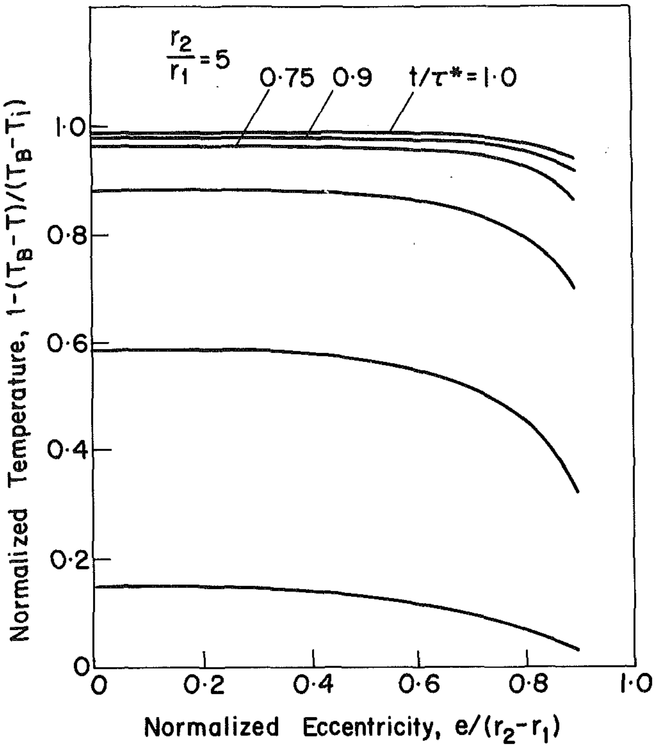


**Fig. 7** Normalized temperature, $\theta$, versus normalized eccentricity, $\epsilon$, for various normalized times, $\tau$, at $r_2/r_1 = 5$

$$\theta = 1 \quad @ \quad \alpha = \alpha_2 \quad \text{(outer surface)}$$

$$\frac{\partial \theta}{\partial R} = 0 \quad @ \quad \alpha = \alpha_1 \quad \text{(bubble surface)}$$

and the initial condition

$$\theta = 0 \quad @ \quad \tau = 0$$

Now, since the flow field is "similar" for the normalized geometric groups, $e/(r_2 - r_1)$ and $r_2/r_1$, and the temperature field is also governed by the same groups according to equations (26) and (18), it is concluded that these groups preserve overall similarity.

## Results and Discussion

The results appearing here were extracted from the computer program. Usually a mesh of $M=31$ by $N=14$ (as described in Fig. 2) gave good results at low and moderate eccentricities. The numerical solution for $\epsilon = 0$ converged exactly to the analytical solution for two concentric cylinders (Ozisik, 1980). At higher eccentricity values, which cause a separated flow regime, a finer mesh was required because of the overcrowding of the streamlines at the left part of the horizontal diameter (see Fig. 1). At $\epsilon = 0.95$ a mesh of $M=99$ and $N=91$ was needed for a correct computation and division of the flow field. But, such a fine mesh requires a very small time increment.

Before discussing the results, one should pay attention to the fact that the coolest point in the fluid is not at the center of the can. In the separated flow regimes the coolest temperature is at the point about which the separated flow rotates. In Fig. 1 this point is marked by an asterisk (*). In the unseparated flow regime the coolest temperature is always at the bubble. In Fig. 5 the transient temperature field is presented for the flow described in Fig. 1. It can be seen that there is a considerable difference between the temperatures of the center and the coolest point.

Figure 6 shows the effect of the bubble location on the coolest temperature point for radii ratio $r_2/r_1 = 5$. It can be seen from the figure that eccentricities ranging from zero (infinite rotating speed) up to $\epsilon_{sep}$, result in the same normalized temperature, $\theta$, as a function of normalized time, $\tau$. Only a drastic increase of the eccentricity causes a lower temperature in the coolest point. This behavior is even more enhanced in the cross-plot shown in Fig. 7, where the normalized temperature is plotted versus the normalized eccentricity at prescribed normalized times. It is obvious that only high eccentricities (0.6 and above) have a pronounced effect on the coolest temperature. It is also clear that the case $\epsilon = 0$ can serve as the upper bound for the temperature at various times.

It is noted that the results in Fig. 7 are presented only up to $\epsilon = 0.9$. Analyzing high eccentricities is costly in computer time, as mentioned earlier, and results may turn out to be meaningless. This is mainly because of the limitation, of the solution given in Gavish et al. (1978), to predict correctly the flow field at high eccentricities, i.e., low rotating speeds. Another limitation of the present analysis is the assumption that the flow and temperature fields are decoupled. This is of course not so since the viscosity is drastically affected by temperature. However, this fact is not very restrictive since a time dependent viscosity results in a time dependent eccentricity. It has been shown, however, that the eccentricity has a weak effect on the temperature (unless the eccentricity reaches high values).

Consider the numerical examples presented in Figs. 1–7:

| | |
|---|---|
| Outer radius, $r_2$, m | 0.045 |
| Bubble radius, $r_1$, m | 0.009 |
| Fluid viscosity, $\mu$, mPa•s | $10^3$ |
| Density, $\rho$, kg/m$^3$ | 900 |
| Specific heat, $c_p$, kJ/kg•°C | 2.0 |
| Thermal conductivity, $k$, W/m•°C | 0.15 |
| Fourier modulus, Fo, | 0.77 |
| Time constant, $\tau^*$, s | 19555 |
| Separation eccentricity, $e$,m, | 0.0107 |
| (Prandtl number, Pr, 13333) | |

It can be seen in Fig. 7 that when $t/\tau^* = 1$, the temperature at the coolest point is just a few percent lower than the surface temperature. Therefore, $\tau^*$, is the time required to reach "almost" steady state.

Similar results, which are not presented here, were generated for the case $r_2/r_1 = 3$. The time constant for $r_2/r_1 = 3$ is about two thirds of that for $r_2/r_1 = 5$, thus requiring much less time to reach steady state.

## Concluding Remarks

A numerical solution is given for the transient temperature distribution in a viscous fluid which fills partially an infinitely long horizontal rotating cylinder. It was found that the coolest temperature is not at the cylinder center, but depends on the flow regime. For unseparated flow it will be on the bubble surface. The bubble eccentricity does not affect considerably the temperature-time dependence. Only at high eccentricity ratios this eccentricity has a profound influence on the temperature – time dependence. The case of $\epsilon = 0$ (no eccentricity, and thus infinitely high rotational speed) is an upper bound for the temperature-time curves.

The results of this analysis were useful in locating the coolest point in the experimental program. The times to reach steady state predicted by the analysis are much larger than those obtained by experiment. This is due to better mixing, which occurs in reality; the model used here is still far from reality, which is much more complex.

## References


Gavish, J., Chadwick, R. S., and Gutfinger, C., 1978, "Viscous Flow in a Partially Filled Rotating Horizontal Cylinder," *Israel Journal of Technology*, Vol. 16, pp. 264–272.

Lenz, M. K., and Lund, D. B., 1978, "The Lethality Fourier Number-Method – Heating Rate Variation and Lethality Confidence Intervals for Forced Convection Heated Food in Containers," *Journal of Food Process Engineering*, Vol. 2, p. 227.

Ozisik, N. N., 1980, *Heat Conduction*, Wiley, New York.